Alanine Scanning Mutagenesis of the Switch I Region in the ATPase Site of *Dictyostelium discoideum* Myosin II[†]

Takashi Shimada, Naoya Sasaki, Reiko Ohkura, and Kazuo Sutoh*

Department of Life Sciences, Graduate School of Arts and Sciences, University of Tokyo, Komaba 3-8-1, Tokyo 153, Japan

Received July 28, 1997; Revised Manuscript Received September 9, 1997[⊗]

ABSTRACT: In order to determine the functional roles of the conserved sequence (NXNSSRFG) of the "switch I" loop (residues 233−240 in *Dictyostelium* myosin II), alanine scanning mutagenesis was performed on *Dictyostelium* myosin II. N233A and S237A mutant myosins did not bind a fluorescent analog of ADP, mant-deoxyADP, at the low concentration range (micromolar and had low level of ATPase activities. They were nonmotile when examined by the *in vitro* motility assay. *Dictyostelium* cells expressing these myosins showed worse phenotypes than that of myosin-null cells. In contrast to these mutant myosins, R238A myosin tightly bound mant-deoxyADP. However, the mutant had a defect in the ATP hydrolysis step and exhibited the lowest ATPase activities among the mutants examined here. The R238A myosin was nonmotile. R238C or R238H mutations, which mimic the Usher syndrome mutations, generated myosins with similar functional defects to those of the R238A mutation. Cells expressing the R238A myosin exhibited the phenotype similar to that of the myosin-null cells. N235A, S236A, F239A, and G240A myosins retained moderate levels of ATPase activities and could drive sliding of actin filaments at various speeds. Phenotypes of cells expressing them were very similar to that of the wild-type cells. Taken together, these results suggest that side chains of N233 and S237 may play essential roles in holding a nucleotide in the ATPase pocket and that R238 may play crucial roles in the ATP hydrolysis step, while those of the other residues in the switch I loop are not essential for the process.

Recently, Rayment et al. determined the crystal structure of the head domain of chicken skeletal myosin (*1*) and also that of the truncated head domain of *Dictyostelium* myosin designated as S1dC (*2*, *3*), which retains motor functions such as actin-activated ATPase activity, actin filament sliding, and force generation (*4*). Comparison of the structures of chicken and *Dictyostelium* myosins revealed that their structures are very similar, though the sequence homology of the head domains of the chicken and *Dictyostelium* myosins is only 47%. Moreover, recent structural studies revealed that the structures of the nucleotide-binding domains of proteins in myosin family, kinesin family, and GTPase family are very similar, indicating that these proteins have evolved from a common ancestor (*5*−*7*).

The ATPase site of myosin is located at the bottom of a deep cleft which splits the central 50 kDa segment into upper and lower domains (the three segments of the S1 heavy chain are traditionally designated as the 25 kDa, 50 kDa, and 20 kDa segments, from the N-terminus). The crystal structure of *Dictyostelium* S1dC complexed with MgADP/BeFx or MgADP/vanadate showed that the bound nucleotide is surrounded by the P-loop (residues 179−186 in *Dictyostelium* myosin II) and two loops in the 50 kDa segment (residues 233−240 and 454−459 in *Dictyostelium* myosin II) (Figure 1). One of the nucleotide-binding loops in the 50 kDa segment of myosin (residues 233−240) is homologous to a loop in the switch I region of GTPases, judging from the topological similarity (*7*). Another loop (residues 454−459) is homologous to the switch II loop of GTPases. The sequence of the former loop of *Dictyostelium* myosin II is NNNSSRFG and is conserved in almost all myosins so far sequenced except the second N (N234). In the crystal structure, the side chain of N233 forms extensive network of hydrogen bonds with phosphate groups of the bound nucleotide. The side chain of N235 is coordinated to α-phosphate group of the nucleotide through a water molecule. The side chain of S236 coordinates to the γ-phosphate and a water molecule and can be involved in ATP hydrolysis (*2*). The side chain of S237 directly coordinates to the Mg ion of the bound nucleotide. In S1dC complexed with MgADP/Vi (*3*), the side chain of R238 forms an ionic bond with that of E459 in the switch II loop to pull the switch II loop closer to the bound nucleotide. The side chains of F239 and G240 are not directly involved in the nucleotide binding, though they may play a role to maintain the overall structure of the ATPase pocket.

Dictyostelium discoideum cells have a single copy of the heavy chain gene of myosin II (*8*). This myosin heavy chain gene has been knocked out by gene replacement (*9*). The resulting myosin-null cells showed characteristic phenotypic defects (*9*−*11*). Moreover, an extrachromosomal vector capable of replicating in *Dictyostelium* cells has been constructed and used for the expression of recombinant myosins in myosin-null cells (*12*, *13*). These powerful genetic tools established by Spudich and his co-workers, enable us to carry out mutational analysis of myosin *in vivo* and *in vitro*. In this study, alanine scanning mutagenesis of

[†] This work was supported by a grant-in-aid by the Ministry of Education, Science and Culture of Japan, and a grant from the International Human Frontier Science Program (HFSP) Organization to K.S.

* To whom correspondence should be addressed.

[⊗] Abstract published in *Advance ACS Abstracts,* November 1, 1997.

[1] Abbreviations: Cy3, sulfoindocyanine; mant, *N*-methylanthraniloyl; S1dC, *Dictyostelium* myosin subfragment 1 with deletion of the C-terminal light chain-binding region.

S0006-2960(97)01837-0 CCC: $14.00

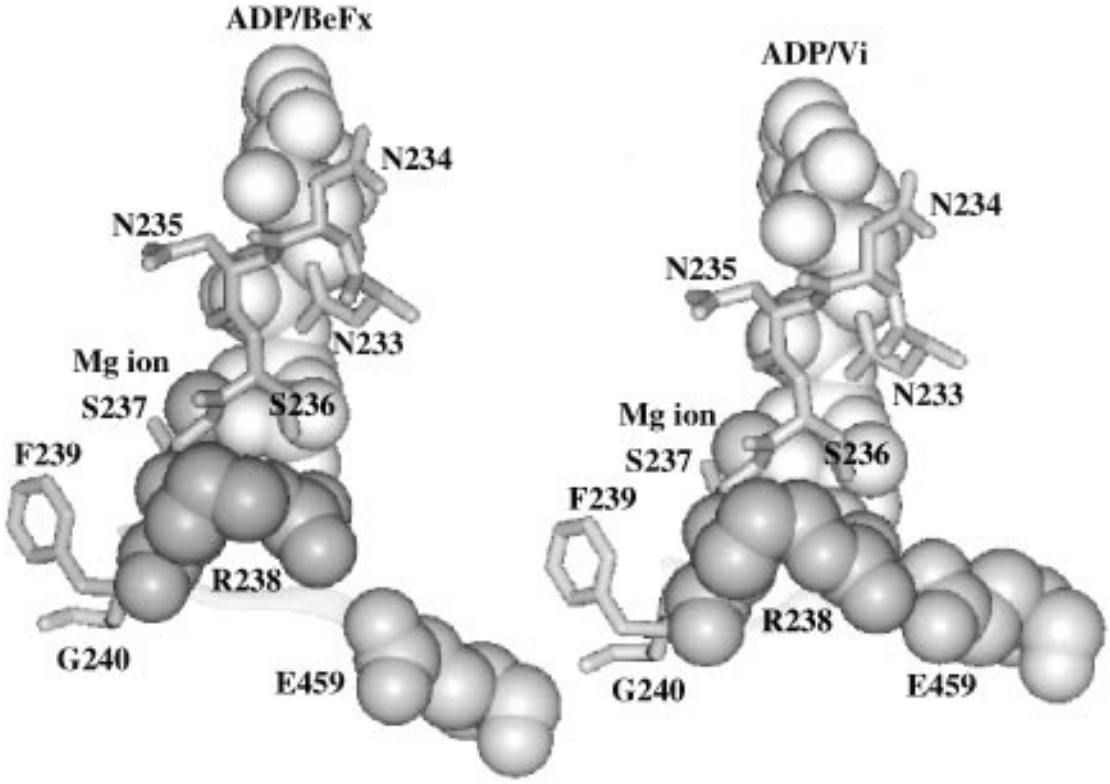

FIGURE 1: The ATPase site of the *Dictyostelium* myosin motor domain (S1dC) complexed with MgADP/BeFx or MgADP/Vi. Residues in the switch I loop (N233−G240) are shown as the stick model (brown) except R238. R238 (brown) and E459 (purple) are shown as the space-filling model. Bound Mg ions (green) and nucleotide analogs (light brown) are also shown as the space-filling model. Note that side chains of R238 and E459 are very close in S1dC complexed with MgADP/Vi.

the residues of the highly conserved switch I loop of myosin comprising from N233 to G240 was carried in order to determine their functions. The effects of these mutations were examined *in vitro* and *in vivo*.

MATERIALS AND METHODS

Construction of Recombinant Myosins. Mutagenesis was carried out by Kunkel's method (*14*). Each residue from N233 to G240 except N234 was changed to alanine by site-directed mutagenesis of the *Dictyostelium* myosin II heavy chain gene (*8*). These mutant myosin heavy-chain genes were ligated into the *Dictyostelium* actin-15 promoter and *Dictyostelium* actin-6 terminator to drive their expression in *Dictyostelium* cells. They were finally inserted into a multicopy extrachromosomal vector, pBIG (*12*), which contains a part of *Dictyostelium* plasmid Ddp1 to ensure extrachromosomal replication (*15*, *16*).

Transformation of Dictyostelium Cells. Plasmids carrying mutant myosin genes were introduced into *Dictyostelium* myosin-null cells in which the myosin II heavy-chain gene was knocked out by homologous recombination (*9*). *Dictyostelium* cells transformed by electroporation (*17*) were selected in HL-5 medium (*18*) supplemented with penicillin/streptomycin and 20 μg/mL of G418 on plastic dishes for a week.

Protein Purification. Myosin preparation was carried out as described previously (*4*) after several modifications. Transformed cells were cultured in suspension or on 220 mm × 220 mm sterile dishes. Approximately 5 g of wet cells was used for each preparation. The following procedure was carried out at 4 °C or on ice. Cells were sonicated in a lysis buffer comprising 10 mM Tris-Cl, pH 7.5, 40 mM sodium pyrophosphate, pH 7.5, 2 mM EDTA, 1 mM dithiothreitol, 0.3 g/mL sucrose, and protease inhibitors, such as leupeptin, pepstatin A, PMSF, and chymostatin. After the addition of 0.3 M KCl, the sonicated cells were centrifuged at 15000*g* for 15 min, and then the supernatant was centrifuged further at 180000*g* for 2 h. The resulting supernatant was dialyzed against a solvent comprising 10 mM MOPS, pH 6.8, 50 mM KCl, 2 mM EDTA, 0.5 mM DTT, and 0.1 mM PMSF. The actomyosin precipitate was collected by centrifugation at 15000*g* for 30 min. Soluble myosin was extracted from the pellet with a solvent comprising 10 mM MOPS, pH 7.4, 0.25 M NaCl, 7 mM $MgCl_2$, and 5 mM ATP. The solution was centrifuged at 560000*g* for 30 min. The supernatant was diluted 5-fold with a kination buffer comprising 10 mM MOPS, pH 7.4, 7 mM $MgCl_2$, 5 mM ATP, and 10 μg/mL recombinant *Dictyostelium* myosin light chain kinase (MLCK) (*12*, *19*). The His-tag MLCK was expressed in *Escherichia coli* and purified on a Ni-NTA column using a gradient of imidazole. The reaction mixture was kept at room temperature for 90 min to allow the phosphorylation reaction to proceed. Then the whole solution was loaded to a HPLC DEAE-5PW column. Myosin was eluted at 0.35 M NaCl. From 5 g of wet cells, 300−500 μg of phosphorylated myosin was obtained. Athough the myosin contains small amount of ADP and/or ATP (approximately micromolar) since they were eluted from the HPLC column at similar salt concentrations, it was used without further purification for ATPase measurements and in vitro motility assays.

For other experiments to use low concentrations of fluorescent nucleotides (mant-deoxyADP and Cy3-ATP), myosin was purified further to remove the contaminating

nucleotides. Myosin eluted from the HPLC column was dialyzed against a solvent comprised of 50 mM NaCl, 10 mM MOPS, pH 6.8, and 5 mM $MgCl_2$ to form filaments. They were collected by centrifugation at 560000*g* for 10 min and then dissolved in 0.35 M NaCl and 10 mM MOPS, pH 7.4

F-actin was extracted from the acetone powder of rabbit skeletal muscle and purified as described previously (*20*).

ATPase Assays. Actin-activated and basal MgATPase activities and high salt CaATPase activity were measured as described previously (*21*) with some modifications. Purified myosin (20−50 μg/mL) and various concentrations of F-actin (0−1 mg/mL) were mixed in an assay buffer comprising 18 mM MOPS, pH 7.4, 12.5 mM KCl, 35 mM NaCl, and 5 mM $MgCl_2$. The reactions were started by adding a 1/10 vol of 10 mM ATP and stopped by adding 4 vol of 0.2 M PCA (perchloric acid). The assays were carried out at 25 °C. The amount of released phosphate was determined as described (*21*). The V_{max} and K_m values were calculated by plotting *V*/*S* vs *S* (*S* is the concentration of actin and *V* is the rate of phosphate release). For these measurements, the wild-type and mutant myosins were prepared at least twice, and the ATPase activities were measured at least three times.

High salt CaATPase activity was measured in an assay buffer comprising 18 mM MOPS, pH 7.4, 0.5 M KCl, 0.1 M NaCl, 5 mM $CaCl_2$, and 1 mM ATP. The reactions were started by adding 20 μg/mL (final concentration) of purified myosin and stopped by adding 19 vol of 0.2 M PCA.

Single Turnover of ATP Hydrolysis. Cy3-ATP (1 μM) was added to the wild-type myosin (0.2 μM) or the R238A myosin (0.5 μM) in 50 mM NaCl, 10 mM MOPS, pH 7.4, and 5 mM $MgCl_2$ at 25 °C. After varying periods of time, a part of the reaction mixture was taken out and mixed with 0.01 vol of PCA to stop the reaction. The resulting solution was centrifuged at 15000 rpm for 10 min to remove insoluble materials. The supernatant was applied directly to a reverse-phase HPLC column (Waters, Nova-pack C18). Elution was carried out by 100 mM potassium phosphate buffer, pH 6.8, 11% acetonitrile. Under the elution conditions, Cy3-ATP and Cy3-ADP were well resolved. Both nucleotides were detected by a fluorometer with a flow cell. Ratio of concentrations of Cy3-ATP and Cy3-ADP was calculated to estimate the amount of the hydrolyzed Cy3-ATP. To compensate the small amount of Cy3-ADP present in the Cy3-ATP preparation as a contaminant, myosin was first mixed with PCA and then mixed with Cy3-ATP. The resulting solution was treated as above.

Binding of mant-deoxyADP. Binding of mant-deoxyADP to myosin was determined in the presence of 0.25 μM of *Dictyostelium* myosin or rabbit skeletal HMM in 150 mM NaCl, 20 mM MOPS, pH 7.4 and 5 mM $MgCl_2$ with varying concentrations of the nucleotide. Under the conditions, *Dictyostelium* myosin II stays in a soluble state. Baseline was determined by using the above solvent without myosin. Fluorescence intensity was measured by Perkin-Elmer LS50B Luminescence Spectrophotometer using excitation at 365 nm and emission at 440 nm. The dissociation constant, K_d, and the number of the bound nucleotide were determined by the Scatchard plot.

In Vitro Motility Assays. *In vitro* motility assays were carried out as previously described (*22*, *23*) with some modifications. Purified myosin (100 μg/mL) was introduced into a chamber constructed from nitrocellulose-coated cover glasses. The assay buffer comprised 25 mM imidazole, pH 7.4, 4 mM $MgCl_2$, 1 mM DTT, 0.2 % of methylcellulose, and O_2 scavengers, such as catalase and glucose oxidase (*24*). F-actin was labeled with rhodamine/phalloidin. Sliding of the fluorescently labeled actin filaments was monitored under a fluorescence microscope equipped with a highly sensitive SIT camera and recorded with a video recorder. The assays were carried out at 25 °C.

Growth Rates of Transformants in Suspension Culture. The growth rates of cells expressing the recombinant myosins were measured in suspension. The HL5 medium contained 10 μg/mL of G418. The inhibitor was shaken at 150 rpm at 22 °C.

Development after Starvation. The development of fruiting bodies by the transformed cells was examined on DM plates covered with a lawn of *Klebsiella aerogenes* (*18*). *Dictyostelium* cells (1.2×10^4) were suspended in 10 mM Tris-Cl, pH 7.5, and then spotted onto the bacterial lawn. When the *Dictyostelium* cells had cleared the bacterial cells, they started to aggregate and to form fruiting bodies. This developmental process was monitored.

RESULTS

Phenotypes of Cells Expressing Recombinant Myosins. Myosin-null cells were transformed with multicopy plasmids carrying mutant myosin genes. After 10−14 days of selection with G418, the phenotypes of the resulting transformants were examined. As previously reported, *Dictyostelium* myosin-null cells grown on a dish can undergo cell division through traction-mediated fission (*10*). Thus, as shown in Figure 2, the phenotype of the myosin-null cells grown on a dish was virtually indistinguishable from that of the wild-type cells (throughout this paper, "the wild-type cells" are myosin-null cells transformed with an extrachromosomal multicopy vector carrying the wild-type myosin II heavy chain gene to express the wild-type myosin II), even though the former cells shows a defect in cytokinesis in suspension culture. Among the transformants, the N235A, S236A, R238A, F239A, and G240A cells grown on dishes exhibited phenotypes very similar to that of the myosin-null cells or wild-type cells (Figure 2). However, the N233A and S237A cells showed very different phenotypes. Many giant cells containing multiple nuclei were observed on culture dishes (Figure 2). Moreover, it took ∼10 days for visible colonies of the N233A or S237A cells to appear on a dish, while it took only 5−7 days for the other transformants, indicating that the cell growth of the former type of transformants was much slower.

The transformants were transferred to suspension culture and their growth rates were monitored. The growth curves of the transformants are shown in Figure 3. The N235A, S236A, F239A, and G240A cells multiplied at the same rate as wild-type cells and reached saturation at 2×10^7 cells/mL. The slow growth of the R238A cells and the myosin-null cells possibly resulted from the breakdown of large, multinuclear cells in suspension. They grew to become giant cells in suspension, and stopped multiplying at the concentration of 5×10^5 cells/mL. The N233A and S237A cells became giant cells in suspension and could not multiply. This observation was consistent with the fact that these two transformants showed severe defects when grown on dishes.

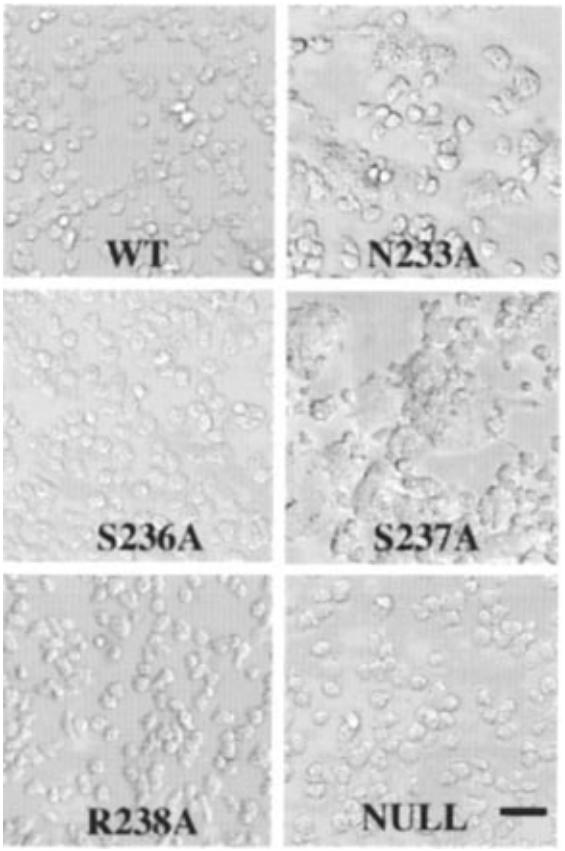

FIGURE 2: Morphology of transformed cells expressing the mutant myosins. As controls, myosin-null cells (NULL) and cells transformed with a plasmid carrying the wild-type myosin heavy chain gene are also shown (WT). The N235A, F239A, and G240A cells were very similar to the wild-type cells. They are not shown here. Cells were grown on plastic dishes for 2 weeks after electroporation. Bar, 25 μm.

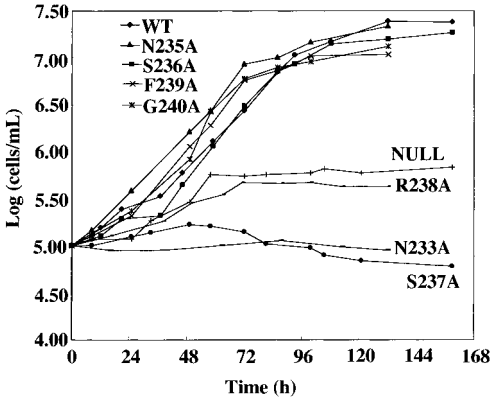

FIGURE 3: Growth of the transformed cells in suspension. As controls, growth of myosin-null cells (NULL) and cells transformed with the plasmid carrying the wild-type myosin heavy chain gene (WT) are also shown. The cells were cultured in suspension on a rotary shaker at 22 °C. The rotation rate was 150 rpm.

The transformants were grown on agar plates covered with a lawn of *K. aerogenes* and were allowed to develop after they had cleared the bacterial cells. The N235A, S236A, F239A, and G240A cells, which grew well in suspension, formed small fruiting bodies with short stalks and often stopped developing at the mound stage, while the N233A, S237A, and R238A cells could not proceed beyond the mound stage just like the myosin-null cells.

ATPase Activities of the Purified Proteins. Transformed cells were cultured on a large scale, and recombinant myosins were purified. During each preparation, myosin was treated with MLCK to phosphorylate the regulatory light chain. Its phosphorylation was confirmed by 2D gel electrophoresis. All of the purified myosins contained normal amounts of regulatory and essential light chains, as judged on SDS gel electrophoresis (data not shown).

Table 1: ATPase Activities of the Wild-Type and Mutant Myosins

mutant myosin	basal MgATPase (s^{-1})	actin-activated MgATPase V_{max} (s^{-1})	actin-activated MgATPase K_m (μM)	Ca-ATPase (s^{-1})
WT	0.062 ± 0.016	2.96 ± 0.08	0.35 ± 0.28	9.80 ± 1.88
N233A	0.026 ± 0.010	0.10 ± 0.03	1.39 ± 1.14	0.16 ± 0.01
N235A	0.046 ± 0.003	2.01 ± 0.44	0.24 ± 0.19	5.03 ± 1.63
S236A	0.042 ± 0.004	0.67 ± 0.01	0.40 ± 0.03	3.50 ± 1.09
S237A	0.018 ± 0.001	0.24 ± 0.06	0.54 ± 0.06	1.04 ± 0.07
R238A	0.010 ± 0.007	0.07 ± 0.04	0.89 ± 0.32	0.14 ± 0.02
R238C	0.007 ± 0.003	0.04 ± 0.02[a]	nd	0.06 ± 0.01
R238H	0.015 ± 0.007	0.08 ± 0.01[a]	nd	0.18 ± 0.01
F239A	0.025 ± 0.001	0.79 ± 0.10	0.65 ± 0.05	1.52 ± 0.10
G240A	0.027 ± 0.010	0.54 ± 0.07	0.43 ± 0.16	0.93 ± 0.07

[a] Actin-activated ATPase activity at 10 μM F-actin.

The actin-activated and basal MgATPase activities of the purified myosins were measured (Table 1). For most of the myosins, the V_{max} value of the actin-activated MgATPase activity was significantly lower than that of the wild-type myosin. Among them, the N233A and R238A myosins exhibited very low V_{max} values (0.10 and 0.07 s^{-1}, respectively) compared to that of the wild-type myosin (2.96 s^{-1}). Their basal MgATPase activities were lower than that of the wild-type myosin (0.062 s^{-1} for the wild-type myosin, 0.026 s^{-1} for the N233A myosin, and 0.007 s^{-1} for the R238A myosin). The V_{max} value of the S237A mutant was slightly higher (0.24 s^{-1}) than that of the N233A or R238A myosin, even though cells expressing this mutant myosin showed the worst phenotype, similar to that of the N233A cells. Its basal MgATPase activity was also low (0.018 s^{-1}). The other mutant myosins, N235A, S236A, F239A, and G240A showed moderate V_{max} values of ~0.5−2.0 s^{-1}. It must be noted here that the V_{max} value of the S236A myosin was 25% of that of the wild-type myosin, though it was proposed that S236 plays a pivotal role in ATP hydrolysis (*2*). The basal MgATPase activities of the N235A, S236A, F239A, and G240A myosins were ~0.03−0.05 s^{-1}. All of the K_m values of the actin-activated ATPase activity were in the similar range for the wild-type and mutant myosins examined here (Table 1).

The CaATPase activities of these mutant myosins in a high ionic strength solvent were also measured (Table 1). Mutant myosins exhibiting lower actin-activated MgATPase activity generally showed lower CaATPase activity. The N233A and R238A myosins had virtually lost their CaATPase activities (0.14 and 0.16 s^{-1} for the mutants; 9.8 s^{-1} for the wild-type myosin).

Titration of mant-deoxyADP Binding. By using a fluorescent ADP analog, mant-deoxyADP, binding of the nucleotide to the wild-type, N233A, S237A, or R238A myosin was measured (Figure 4). As a control, binding of mant-deoxyADP to rabbit skeletal HMM was also measured. The N233A and S237A myosins did not bind the fluorescent nucleotide at low concentrations, while the R238A myosin bound it more tightly than the wild-type myosin. Dissociation constant, K_d, of mant-deoxyADP was calculated as 1.9 μM to the *Dictyostelium* wild-type myosin, and 0.4 μM to

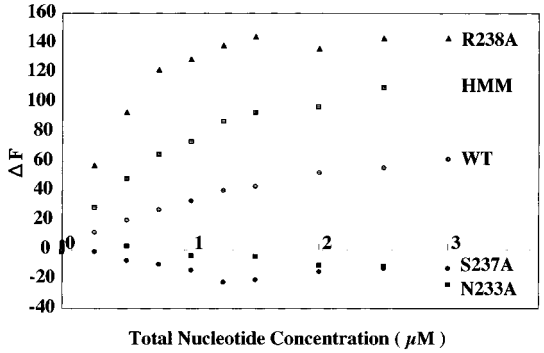

FIGURE 4: Binding of mant-deoxyADP to the wild-type and mutant myosins. As a control, binding of the nucleotide to rabbit skeletal HMM was also measured. Conditions: myosin or HMM, 0.25 μM; solvent, 150 mM NaCl, 20 mM MOPS, pH 7.4, 5 mM $MgCl_2$, and varying concentrations of mant-deoxyADP. ΔF is the difference of the fluorescence intensity in the presence of myosin or HMM and that in their absence.

rabbit skeletal HMM, while the binding was tighter to the R238A myosin (K_d, 0.1 μM). Maximum number of the bound mant-deoxyADP was 1.1 mol/mol of the ATPase site for the wild-type myosin, 1.0 mol/mol for rabbit HMM, and 1.1 mol/mol for the R238A myosin. Even though we could not detect any appreciable binding of mant-deoxyADP to the N233A and S237A myosins at the low concentration range examined here, it seems that these mutant myosins can bind MgATP at much higher concentrations, considering the facts that during the preparation the N233A and S237A myosin molecules were extracted from the actomyosin precipitate by MgATP and that the S237A myosin retained low but appreciable level of the actin-activated MgATPase and CaATPase activities.

Single Turnover of ATP Hydrolysis. Since the R238A myosin bound mant-deoxyADP tightly, it seems that virtual loss of the ATPase activity by the mutation resulted from a defect in the ATP hydrolysis step or in the P_i release step of the ATPase cycle. To determine which step was blocked by the mutation, we examined if the mutant myosin quickly hydrolyses ATP at the first cycle as the wild-type myosin by using a highly fluorescent ATP analog, Cy3-ATP. It was previously shown that myosin can hydrolyze Cy3-ATP (*25*). The first cycle of hydrolysis of the ATP analog, i.e., the single turnover, was followed by incubating myosin with an equimolar or slightly excess amount of Cy3-ATP. When the wild-type myosin was incubated with Cy3-ATP, ~0.7 mol of the ATP analogs/mol of ATPase site was quickly hydrolyzed to generate Cy3-ADP, and then much slower hydrolysis was followed (Figure 5). This "ADP burst" reflected the first, quick cycle of ATP hydrolysis. Much slower hydrolysis followed the ADP burst because the P_i release became the rate-limiting step once the ATPase site was occupied by ADP/P_i to form the stable myosin/ADP/P_i intermediate. Contrary to the hydrolysis of Cy3-ATP by the wild type myosin, the R238A myosin did not show any ADP burst. No appreciable hydrolysis of Cy3-ATP was observed for a prolonged period of time, indicating that the R238A mutation blocked the ATP hydrolysis step, not the P_i release step.

In Vitro Motility Assays. *In vitro* motility assays were carried out on the purified myosins (Figure 6). The N235A, S236A, F239A, and G240A myosins could drive sliding of actin filaments, although much more slowly than the wild-type myosin. Among them, the G240A myosin exhibited the slowest sliding motion. The N233A, S237A, and R238A myosins could not drive the sliding of actin filaments. When MgATP was added, rhodamine-labeled actin filaments on a glass surface covered with the R238A myosin did not show any directional movement, and the actin filaments started to exhibit Brownian motion away from the glass surface. Fluorescent actin filaments on the N233A and S237A myosins, however, did not show Brownian motion in the presence of ATP, it appearing as if they were fixed on myosins through rigor bonds.

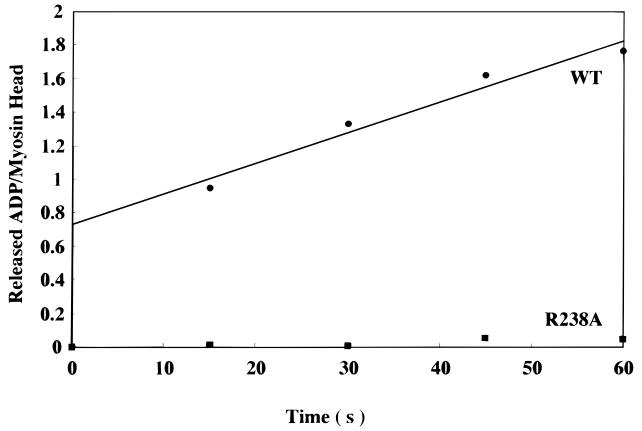

FIGURE 5: Hydrolysis of Cy3-ATP by the wild-type and R238A myosin. The wild-type myosin (0.2 μM) or the R238A myosin (0.5 μM) was mixed with Cy3-ATP (1 μM) in 50 mM NaCl, 10 mM MOPS, pH 7.4, and 1 mM $MgCl_2$ at 25 °C. Amounts of the hydrolyzed Cy3-ATP were determined by a reversed-phase HPLC and plotted against reaction times. It is apparent that the wild-type myosin exhibited the "ADP burst" while the R238A myosin did not.

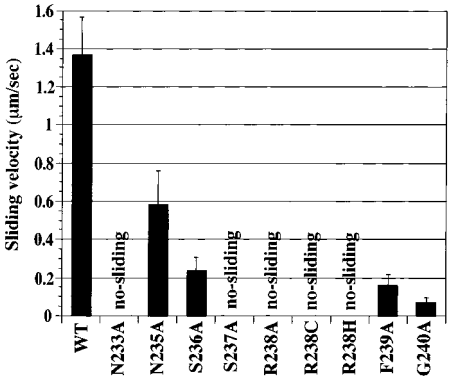

FIGURE 6: Sliding velocity of actin filaments on the mutant myosins. Motility assays were carried out on a nitrocellulose-coated glass surface at 25 °C. When actin filaments did not exhibit any directional motion on mutant myosin molecules, it is indicated as "no-sliding". For the nonmotile R238A myosin, actin filaments dissociated from the glass surface on the addition of MgATP through Brownian motion, while the filaments stayed on the glass surface when the N233A and S237A mutants were used.

Inhibition of the Filament Sliding by Mutant Myosins. Judging from the above results, it seems that the N233A and S237A myosins mostly remain in the strong-binding state, while the R238A myosin is in the weak-binding state during the ATP hydrolysis cycle. In order to determine if this is the case, *in vitro* motility assays were carried out on mixtures of the wild-type myosin and the N233A, S237A or R238A myosin in varying ratios. As shown in Figure 7, the sliding of actin filaments driven by the wild-type myosin was completely inhibited on the addition of small amount of the

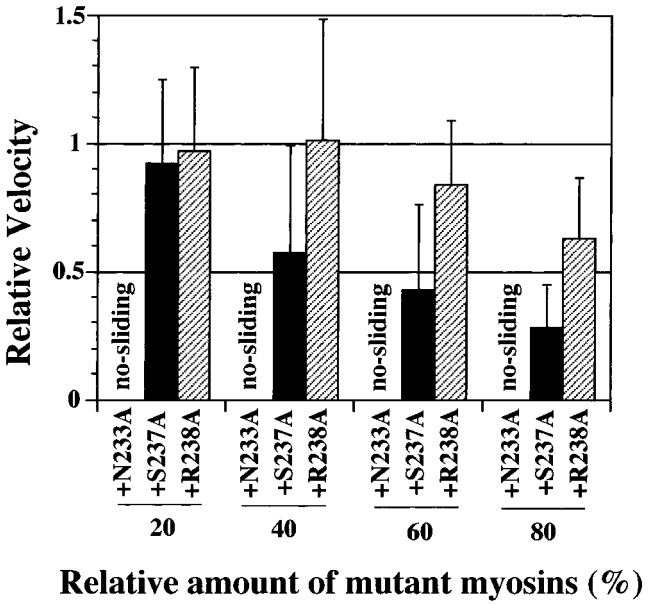

FIGURE 7: Sliding velocity of actin filaments on a mixture of the wild-type myosin and one of the mutant myosins (N233A, S237A, or R238A myosin). The total amount of myosins was kept constant, while the ratio of the wild-type myosin and the mutant myosin was changed. Measurements were carried out as in Figure 6.

N233A myosin (20% of the total myosin). The S237A myosin also exerted an inhibitory effect on the sliding motion of actin filaments driven by the wild-type myosin. The rate of filament sliding on the wild-type/S237A mixture was proportional to the amount of the wild-type myosin. Unlike these two mutant myosins, the inhibitory effect of the R238A myosin became obvious only when a much higher concentration of the mutant myosin was present in the mixture.

Usher Syndrome Mutations in Dictyostelium Myosin. It was reported that mutations of arginine to cysteine and arginine to histidine in human myosin VIIA at the site corresponding to R238 in *Dictyostelium* myosin are responsible for Usher syndrome type 1B, an inherited disease associated with human deafness (*26*). Since the NXNSSRFG sequence of the switch I loop is highly conserved in myosins so far sequenced, including human myosin VIIA, and since it is very likely that the three-dimensional structure around the loop in the ATPase pocket is very similar in *Dictyostelium* myosin II and human myosin VIIA, the R238C and R238H mutations introduced into *Dictyostelium* myosin II would functionally mimic the Usher syndrome mutations in the human myosin. When the R238C or R238H myosin was expressed in *Dictyostelium* myosin-null cells, the phenotypes of the transformants were the same as that of the cells expressing the R238A myosin (data not shown). The actin-activated and basal MgATPase activities were virtually abolished by the R238C or R238H mutation (Table 1). The CaATPase activity was also virtually abolished by the mutations (Table 1). Actin filaments did not slide on these mutant myosins (Figure 6).

DISCUSSION

The side chain of N233 interacts extensively with an ATP molecule, coordinating to ribose and α-, β-, γ-phosphate group (*2*, *3*). The side chain of S237 coordinates to the Mg ion of MgADP/BeFx and MgADP/vanadate bound in the ATPase pocket. Thus, it is expected that replacement of N233 or S237 with alanine would significantly weaken the binding of MgATP or MgADP in the ATPase pocket. In fact, mant-deoxyADP, a fluorescent analog of MgADP, did not bind to the N233A and S237A myosins at the low concentration range of the nucleotide, and these myosins exhibited low level of the MgATPase and CaATPase activities. Consistent with the observations, the N233A and S237A myosins not only lost the ability to drive sliding of actin filaments, but also inhibited the sliding driven by the wild-type myosin, an indication that some of myosin molecules form rigor-like bonds with actin filaments even in the presence of MgATP. The rigor-like bonds with microfilaments in the transformed cells would result in much worse phenotypes than that of the myosin-null cells.

Here, it is assumed that the N233A and S237A mutations disrupt the specific bonds with the bound nucleotide, resulting in the observed loss of the *in vitro* and *in vivo* motor activities. However, we cannot exclude another possibility that these mutations simply disrupted the three-dimensional structure of the ATPase pocket in a nonspecific way to induce the observed effects. This possibility is less likely for the S237A mutant, considering the fact that the myosin retained a low but an appreciable level of the actin-activated ATPase activity and the CaATPase activity. The more straightforward answer would be obtained by crystallographic studies on these mutants.

The R238A myosin exhibited the lowest actin-activated and basal MgATPase activities. It also exhibited the lowest CaATPase activity. The myosin tightly bound mant-deoxyADP, implying that, unlike the N233A or S237A mutation, the R238A mutation did not block the binding of a nucleotide. The single turnover experiment using Cy3-ATP indicated that the ATP hydrolysis step is blocked by the mutation. In the crystal structure of S1dC complexed with MgADP/Vi (*3*), the switch II loop comprised of residues 454−459 is close to the ATPase site in such a way that the side chain of R238 forms an ionic bond with that of E459. The side chain of E459 is then hydrogen bonded to a water molecule which is supposed to be closely located to the γ-phosphate of the bound ATP. It must be mentioned here that the E459A mutation generated the same defect as the R238A mutation (manuscript in preparation). Therefore, it seems that the structure of the ATPase site maintained by the R238−E459 interaction is prerequisite for the ATP hydrolysis step.

The notion that the R238A mutation blocked the ATP hydrolysis step is consistent with phenotypes of the transformed cells expressing the mutant myosin. Since the R238A myosin would remain in the weak binding state, it is expected that the transformed cells behave like myosin-null cells, even though the mutation abolished all motor functions.

When R238 was replaced with cysteine or histidine in *Dictyostelium* myosin II to mimic the Usher syndrome mutations of human myosin VIIA, the resulting R238C and R238H myosins exhibited the same behavior as that of the R238A myosin *in vivo* and *in vitro*. Since the sequence NXNSSRFG in the switch I loop is highly conserved among myosins, this result implies that the Usher syndrome mutations in human myosin VIIA would result in virtual loss of ATPase activity due to the block of the ATP hydrolysis step, and therefore in loss of other motor functions.

Although N235, S236, F239, and G240 are conserved in every myosin so far sequenced, including *Drosophila* ninaC, replacement of these residues with alanine did not eliminate the motor functions. These mutant myosins retained the actin-activated MgATPase activity; their V_{max} values ranged from ~0.5 s^{-1} to ~2.0 s^{-1}. They also drove sliding of actin filaments; although, the sliding velocity was very low for the G240A myosin. Thus, N235, S236, F239, and G240 are not essential for ATP hydrolysis or the motor functions triggered by the hydrolysis.

For the hydrolysis of ATP, a proton must be transferred from a water molecule to the γ-phosphate. It was proposed that the hydroxyl group of S236 serves as an intermediate for transferring the proton from the water to the γ-phosphate group (*2*). Replacement of S236 with alanine, however, did not eliminate the ATPase activities or other motor functions. The S236A myosin still retained actin-activated ATPase activity. The V_{max} value of the mutant was 25% of that of the wild-type myosin (2.96 s^{-1} vs 0.67 s^{-1}). The mutant myosins could drive sliding of actin filaments, though at slower rate than the wild-type myosin (1.4 μm/s vs 0.2 μm/s). Thus, it seems unlikely that S236 is the key residue for the ATP hydrolysis.

N235, F239, and G240 are not directly involved in the nucleotide binding of S1dC complexed with MgADP/BeFx or MgADP/Vi (*2*, *3*) and may play a role in maintaining the overall structure of the ATPase pocket. Consistent with this notion, the mutations on these residues hampered, but did not eliminate, the motor functions. It must be noted here that even while the sliding velocity is very slow (0.07 μm/s) and the actin-activated ATPase activity is also low (V_{max}, 0.54 s^{-1}) compared to those of the wild-type myosin (velocity, 1.4 μm/s; V_{max}, 2.96 s^{-1}), the G240A myosin can still retain its *in vivo* functions, as judged from the observation that cells expressing this mutant myosin could grow in suspension at the same rate as ones expressing the wild-type myosin, and that they formed fruiting bodies, although the development often stopped at the mound stage.

In summary, alanine scanning mutagenesis of the switch I loop of *Dictyostelium* myosin II showed: (1) N233 and S237 may play essential roles in holding a nucleotide in the ATPase pocket, (2) R238 is essential for the ATP hydrolysis step possibly because the R238−E459 ionic bond maintains the conformation necessary for the step, (3) S236 may not be directly involved in ATP hydrolysis, and (4) N235, F239, and G240 may play roles to maintain the overall structure of the ATPase pocket.

ACKNOWLEDGMENT

The coordinates of the motor domain of *Dictyostelium* myosin II were kindly provided by Dr. I. Rayment (University of Wisconsin). The myosin II heavy chain gene, myosin-null cell, pBIG vector, and recombinant MLCK gene were kindly supplied by Dr. J. A. Spudich (Stanford University), Dr. B. Patterson (University of Arizona), and Dr. T. Q. P. Uyeda (National Institute for Advanced Interdisciplinary Research, Japan). mant-deoxyADP was synthesized and supplied by Dr. T. Hiratsuka (Asahikawa Medical University). Cy3-ATP was synthesized and supplied by Dr. K. Oiwa (Kansai Advanced Research Center, Japan). We also thank Dr. Ivan Rayment for discussions for various parts of this paper.

REFERENCES

1. Rayment, I., Rypniewski, W. R., Schmidt, B. K., Smith, R., Tomchick, D. R., Benning, M. M., Winkelmann, D. A., Wesenberg, G., and Holden, H. M. (1993) *Science 261*, 50−58.
2. Fisher, A. J., Smith, C. A., Thoden, J. B., Smith, R., Sutoh, K., Holden, H. M., and Rayment I. (1995) *Biochemistry 34*, 8960−8972.
3. Smith, C. A., and Rayment, I. (1996) *Biochemistry 35*, 5404−5417.
4. Itakura, S., Yamakawa, H., Toyoshima, Y. Y., Ishijima, A., Kojima, T., Harada, Y., Yanagida, T., Wakabayashi, T., and Sutoh, K. (1993) *Biochem. Biophys. Res. Commun. 196*, 1504−1510.
5. Kull, F. J., Sablin, E. P., Lau, R., Fletterick, R. J., and Vale, R. D. (1996) *Nature 380*, 550−555.
6. Sablin, E. P., Kull, F. J., Cooke, R., Vale, R. D., and Fletterick, R. J. (1996) *Nature 380*, 555−559.
7. Smith, C. A., and Rayment, I. (1996) *Biophys. J. 70*, 1590−1602.
8. DeLozanne, A., Lewis, M., Spudich, J. A., and Leinwand, L. A. (1985) *Proc. Natl. Acad. Sci. U.S.A. 82*, 6807−6810.
9. Manstein, D. J., Titus, M. A., De, L. A., and Spudich, J. A. (1989) *EMBO J. 8*, 923−932.
10. DeLozanne, A., and Spudich, J. A. (1987) *Science 236*, 1086−1091.
11. Knecht, D. A., and Loomis, W. F. (1987) *Science 236*, 1081−1086.
12. Ruppel, K. M., Uyeda, T. Q., and Spudich, J. A. (1994) *J. Biol. Chem. 269*, 18773−18780.
13. Uyeda, T. Q. P., Ruppel, K. M., & Spudich, J. A. (1994) *Nature 368*, 567−569.
14. Kunkel, T. A. (1985) *Proc. Natl. Acad. Sci. U.S.A. 82*, 488−492.
15. Firtel, R. A., Silan, C., Ward, T. E., Howard, P., Metz, B. A., Nellen, W., and Jacobson, A. (1985) *Mol. Cell Biol. 5*, 3241−3250.
16. Noegel, A., Welker, D. L., Metz, B. A., and Williams, K. L. (1985) *J. Mol. Biol. 185*, 447−450.
17. Howard, P. K., Ahern, K. G., and Firtel, R. A. (1988) *Nucleic Acids Res. 16*, 2613−2623.
18. Sussman, M. (1987) *Methods Cell Biol. 28*, 9−29.
19. Tan, J. L., and Spudich, J. A. (1991) *J. Biol. Chem. 266*, 16044−16049.
20. Spudich, J. A., and Watt, S. (1971) *J. Biol. Chem. 246*, 4866−4871.
21. Kodama, T., Fukui, K., and Kometani, K. (1986) *J. Biochem. (Tokyo) 99*, 1465−1472.
22. Kron, S. J., and Spudich, J. A. (1986) *Proc. Natl. Acad. Sci. U.S.A. 83*, 6272−6276.
23. Toyoshima, Y. Y., Kron, S. J., MacNally, E. M., Niebling, K. R., Toyoshima, C., and Spudich, J. A. (1987) *Nature 328*, 536−539.
24. Harada, Y., Sakurada, K., Aoki, T., Thomas, D. D., and Yanagida, T. (1990) *J. Mol. Biol. 216*, 49−68.
25. Funatsu, T., Harada, Y., Tokunaga, M., Saito, K., and Yanagida, T. (1995) *Nature 374*, 555−559.
26. Weil, D., Blanchard, S., Kaplan, J., Guilford, P., Gilson, P., Wlash, J., Mburu, P., Varela, A., Levilliers, J., Weston, M. D., Kelly, P. M., Kimberling, W. J., Wagenaar, M., Levi-Acobas, F., Larget-Piet, D., Munnich, A., Steel, K. P., Brown, S. D., M., and Petit, C. (1995) *Nature 374*, 60−61.

BI971837I